Edge-Unfolding Nearly Flat Convex Caps

Joseph O'Rourke
Smith College, Department of Computer Science
Northampton, MA, USA
jorourke@smith.edu
https://orcid.org/0000-0001-5844-506X

Abstract

The main result of this paper is a proof that a nearly flat, acutely triangulated convex cap $\mathcal{C}$ in $\mathbb{R}^3$ has an edge-unfolding to a non-overlapping polygon in the plane. A *convex cap* is the intersection of the surface of a convex polyhedron and a halfspace. "Nearly flat" means that every outer face normal forms a sufficiently small angle $\phi < \Phi$ with the $\hat{z}$-axis orthogonal to the halfspace bounding plane. The size of Φ depends on the acuteness gap α: if every triangle angle is at most $\pi/2-\alpha$, then $\Phi \approx 0.36\sqrt{\alpha}$ suffices; e.g., for $\alpha = 3°$, $\Phi \approx 5°$. The proof employs the recent concepts of angle-monotone and radially monotone curves. The proof is constructive, leading to a polynomial-time algorithm for finding the edge-cuts, at worst $O(n^2)$; a version has been implemented.

2012 ACM Subject Classification Theory of computation → Computational geometry, Mathematics of computing → Graph theory

Keywords and phrases polyhedra, unfolding

Digital Object Identifier 10.4230/LIPIcs.SoCG.2018.64

Related Version A full version of this paper is available at [13], `http://arxiv.org/abs/1707.01006`.

Acknowledgements I benefited from discussions with Anna Lubiw and Mohammad Ghomi. I am grateful to four anonymous referees, who found an error in Lemma 5 and offered an alternative proof, shortened the justifications for Lemmas 3 and 6, suggested extensions and additional relevant references, and improved the exposition throughout.

1 Introduction

Let $\mathcal{P}$ be a convex polyhedron in $\mathbb{R}^3$, and let $\phi(f)$ be the angle the outer normal to face f makes with the $\hat{z}$-axis. Let H be a halfspace whose bounding plane is orthogonal to the $\hat{z}$-axis, and includes points vertically above that plane. Define a *convex cap* $\mathcal{C}$ of angle Φ to be $\mathcal{C} = \mathcal{P} \cap H$ for some $\mathcal{P}$ and H, such that $\phi(f) \leq \Phi$ for all f in $\mathcal{C}$. We will only consider $\Phi < 90°$, which implies that the projection C of $\mathcal{C}$ onto the xy-plane is one-to-one. Note that $\mathcal{C}$ is not a closed polyhedron; it has no "bottom," but rather a boundary $\partial\mathcal{C}$.

Say that a convex cap $\mathcal{C}$ is *acutely triangulated* if every angle of every face is strictly acute, i.e., less than 90°. It may be best to imagine first constructing $\mathcal{P} \cap H$ and then acutely triangulating the surface. That every polyhedron may be acutely triangulated was first established by Burago and Zalgaller [4]. Recently Bishop proved that every PSLG (planar straight-line graph) of n vertices has a conforming acute triangulation, using $O(n^{2.5})$ triangles [2].[1] Applying Bishop's algorithm will create edges with flat (π) dihedral angles,

[1] His main Theorem 1.1 is stated for non-obtuse triangulations, but he says later that "the theorem also holds with an acute triangulation, at the cost of a larger constant in the $O(n^{2.5})$."

34th International Symposium on Computational Geometry (SoCG 2018).
Editors: Bettina Speckmann and Csaba D. Tóth; Article No. 64; pp. 64:1–64:14
Leibniz International Proceedings in Informatics
LIPICS Schloss Dagstuhl – Leibniz-Zentrum für Informatik, Dagstuhl Publishing, Germany

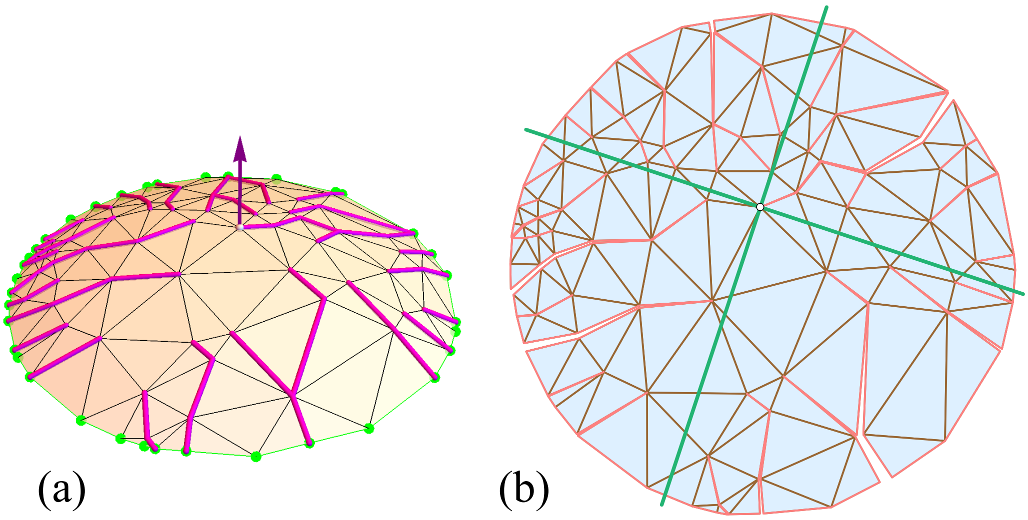

Figure 1 (a) A convex cap of 98 vertices, $\Phi \approx 33°$, with spanning forest $\mathcal{F}$ marked. $\mathcal{C}$ is non-obtusely triangulated (rather than acutely triangulated). (b) Edge-unfolding by cutting $\mathcal{F}$. The quadrant lines are explained in Section 5.2.

resulting from partitioning an obtuse triangle into several acute triangles. One might view the acuteness assumption as adding extra possible cut edges.

An *edge-unfolding* of a convex cap $\mathcal{C}$ is a cutting of edges of $\mathcal{C}$ that permits $\mathcal{C}$ to be developed to the plane as a simple (non-self-intersecting) polygon, a "net." The cut edges must form a boundary-rooted spanning forest $\mathcal{F}$: a forest of trees, each rooted on the boundary rim $\partial\mathcal{C}$, and spanning the internal vertices of $\mathcal{C}$. Our main result is:

▶ **Theorem 1.** *Every acutely triangulated convex cap $\mathcal{C}$ with face normals bounded by a sufficiently small angle Φ from the vertical, has an edge-unfolding to a non-overlapping polygon in the plane. The angle Φ is a function of the acuteness gap α (Eq. 6). The cut forest can be found in quadratic time.*

An example is shown in Fig. 1. Even if $\mathcal{C}$ is closed to a polyhedron by adding the convex polygonal base under $\mathcal{C}$, this polyhedron can be edge-unfolded without overlap [12].

1.1 Background

It is a long standing open problem whether or not every convex polyhedron has a non-overlapping edge-unfolding, often called Dürer's problem [6] [10]. Theorem 1 can be viewed as an advance on a narrow version of this problem. This theorem – without the acuteness assumption – has been a folk-conjecture for many years. A specific line of attack was conjectured in [9], and it is that sketch I follow for the proof here.

There have been two recent advances on Dürer's problem. The first is Ghomi's positive result that sufficiently thin polyhedra have edge-unfoldings [7]. This can be viewed as a counterpart to Theorem 1, which when supplemented by [12] shows that sufficiently flat polyhedra have edge-unfoldings. The second is a negative result that shows that when restricting cutting to geodesic "pseudo-edges" rather than edges of the polyhedral skeleton, there are examples that cannot avoid overlap [1].

It is natural to hope that Theorem 1 might lead to an edge-unfolding result for all acutely triangulated convex polyhedra, but I have been so far unsuccessful in realizing this hope. Possible extensions are discussed in Section 11.

2 Overview of algorithm

We now sketch the simple algorithm in four steps; the proof of correctness will occupy the remainder of the paper. First, $\mathcal{C}$ is projected orthogonally to C in the xy-plane, with Φ small enough so that the acuteness gap of $\alpha > 0$ decreases to $\alpha' \leq \alpha$ but still $\alpha' > 0$. So C is acutely triangulated. Second, a boundary-rooted angle-monotone spanning forest F for C is found using the algorithm in [9]. Both the definition of angle-monotone and the algorithm will be described in Section 5 below, but for now we just note that each leaf-to-root path in F is both x- and y-monotone in a suitably rotated coordinate system. Third, F is lifted to a spanning forest $\mathcal{F}$ of $\mathcal{C}$, and the edges of $\mathcal{F}$ are cut. Finally, the cut $\mathcal{C}$ is developed flat in the plane. In summary: project, lift, develop.

I have not pushed on algorithmic time complexity, but certainly $O(n^2)$ suffices, as detailed in the full version [13].

3 Overview of proof

The proof relies on two results from earlier work: the angle-monotone spanning forest result in [9], and a radially monotone unfolding result in [11]. Those results are revised and explained as needed to allow this paper to stand alone. It is the use of angle-monotone and radially monotone curves and their properties that constitute the main novelties. The proof outline has these seven high-level steps, expanding upon the algorithm steps:

1. Project $\mathcal{C}$ to the plane containing its boundary rim, resulting in a triangulated convex region C. For sufficiently small Φ, C is again acutely triangulated.
2. Generalizing the result in [9], there is a θ-angle-monotone, boundary-rooted spanning forest F of C, for $\theta < 90°$. F lifts to a spanning forest $\mathcal{F}$ of the convex cap $\mathcal{C}$.
3. For sufficiently small Φ, both sides L and R of each cut-path $\mathcal{Q}$ of $\mathcal{F}$ are θ-angle-monotone when developed in the plane, for some $\theta < 90°$.
4. Any planar angle-monotone path for an angle $\leq 90°$, is radially monotone, a concept from [11].
5. Radial monotonicity of L and R, and sufficiently small Φ, imply that L and R do not cross in their planar development. This is a simplified version of a result from [11], and here extended to trees.
6. Extending the cap $\mathcal{C}$ to an unbounded polyhedron $\mathcal{C}^\infty$ ensures that the non-crossing of each L and R extends arbitrarily far in the planar development.
7. The development of $\mathcal{C}$ can be partitioned into θ-monotone "strips," whose side-to-side development layout guarantees non-overlap in the plane.

Through sometimes laborious arguments, I have tried to quantify steps even if they are in some sense obvious. Various quantities go to zero as $\Phi \to 0$. Those laborious arguments and other details are can be found in the full version [13].

3.1 Notation

I attempt to distinguish between objects in $\mathbb{R}^3$, and planar projected versions of those objects, either by using calligraphy ($\mathcal{C}$ in $\mathbb{R}^3$ vs. C in $\mathbb{R}^2$), or primes (γ in $\mathbb{R}^3$ vs. γ' in $\mathbb{R}^2$), and occasionally both ($\mathcal{Q}$ vs. Q'). Sometimes this seems infeasible, in which case we use different symbols (u_i in $\mathbb{R}^3$ vs. v_i in $\mathbb{R}^2$). Sometimes we use $\perp$ as a subscript to indicate projections or developments of lifted quantities.

4 Projection angle distortion

> 1. Project $\mathcal{C}$ to the plane containing its boundary rim, resulting in a triangulated convex region C. For sufficiently small Φ, C is again acutely triangulated.

This first claim is obvious: Since every triangle angle is strictly less than 90°, and the distortion due to projection to a plane goes to zero as $\mathcal{C}$ becomes more flat, for some sufficiently small Φ, the acute triangles remain acute under projection.

In order to obtain a definite dependence on Φ, the following exact bound is derived in the full version [13].

▶ **Lemma 2.** *The maximum absolute value of the distortion $\Delta_\perp$ of any angle in $\mathbb{R}^3$ projected to the xy-plane, with respect to the tilt ϕ of the plane of that angle with respect to z, is given by:*

$$\Delta_\perp(\phi) \ = \ \cos^{-1}\left(\frac{\sin^2\phi}{\sin^2\phi - 2}\right) - \pi/2 \ \approx \ \phi^2/2 - \phi^4/12 + O(\phi^5) \ , \tag{1}$$

where the approximation holds for small ϕ.

In particular, $\Delta_\perp(\Phi) \to 0$ as $\Phi \to 0$. For example, $\Delta_\perp(10°) \approx 0.9°$.

5 Angle-monotone spanning forest

> 2. Generalizing the result in [9], there is a θ-angle-monotone, boundary rooted spanning forest F of C, for $\theta < 90°$. F lifts to a spanning forest $\mathcal{F}$ of the convex cap $\mathcal{C}$.

First we define angle-monotone paths, which originated in [5] and were further explored in [3], and then turn to the spanning forests we need here.

5.1 Angle-monotone paths

Let C be a planar, triangulated convex domain, with ∂C its boundary, a convex polygon. Let G be the (geometric) graph of all the triangulation edges in C and on ∂C.

Define the *θ-wedge* $W(\theta, v)$ to be the region of the plane bounded by rays separated by angular *width* θ emanating from v in fixed directions. W is closed along (i.e., includes) both rays. A polygonal path $Q = (v_0, \ldots, v_k)$ following edges of G is called *θ-angle-monotone* (or *θ-monotone* for short) if the vector of every edge (v_i, v_{i+1}) lies in $W(\theta, v_0)$ (and therefore $Q \subseteq W(\theta, v_0)$) in a fixed coordinate system.[2] If $\theta \leq 90°$, then a θ-monotone path is both x- and y-monotone in a suitable coordinate system, i.e., it meets every vertical, and every horizontal line in a point or a segment, or not at all.

[2] My notation here is slightly different from the notation in [9] and earlier papers, as I want to emphasize the reliance on θ.

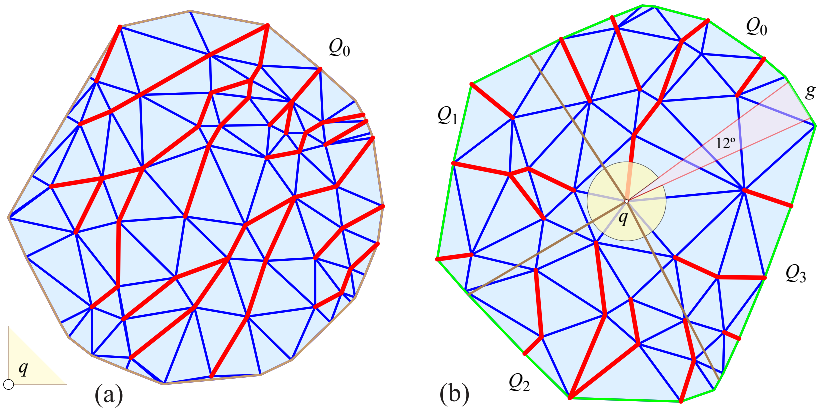

Figure 2 (a) q placed so that $C \subset Q_0$. (b) near-quadrants Q_i have width $\theta = 87°$, so the gap g has angle $4\alpha' = 12°$.

5.2 Angle-monotone spanning forest

It was proved in [9] that every non-obtuse triangulation G of a convex region C has a boundary-rooted spanning forest F of C, with all paths in F 90°-monotone. We describe the proof and simple construction algorithm before detailing the changes necessary for strictly acute triangulations.

Some internal vertex q of G is selected, and the plane partitioned into four 90°-quadrants Q_0, Q_1, Q_2, Q_3 by orthogonal lines through q. Each quadrant is closed along one axis and open on its counterclockwise axis; q is considered in Q_0 and not in the others, so the quadrants partition the plane. Then paths are grown within each quadrant independently, as follows. A path is grown from any vertex $v \in Q_i$ not yet included in the forest F_i, stopping when it reaches either a vertex already in F_i, or ∂C. These paths never leave Q_i, and result in a forest F_i spanning the vertices in Q_i . No cycle can occur because a path is grown from v only when v is not already in F_i; so v becomes a leaf of a tree in F_i. Then $F = F_1 \cup F_2 \cup F_3 \cup F_4$.

Because our acute triangulation is a non-obtuse triangulation, following the algorithm from [9] leads to angle-monotone paths for $\theta = 90° - \alpha' < 90°$. Although it is natural to place the quadrants origin q near the center of C, in fact choosing a q exterior to C so that all paths fall in the near-quadrant Q_0 suffices to determine F; see Fig. 2(a). The only reason to prefer a $q \in C$ is that this allows the conclusion mentioned earlier that closing $\mathcal{C}$ with a convex polygon base still permits an edge-unfolding of the closed polyhedron [12]. We leave the argument that shows q can be chosen at an interior vertex of C (see Fig. 2(b)) to the full version [13], and continue to illustrate $q \in C$.

We conclude this section with a lemma:

▶ **Lemma 3.** *If G is an acute triangulation of a convex region C, with acuteness gap α', then there exists a boundary-rooted spanning forest F of C, with all paths in F θ-angle-monotone, for $\theta = 90° - \alpha' < 90°$.*

6 Curve distortion

3. For sufficiently small Φ, both sides L and R of each cut-path $\mathcal{Q}$ of $\mathcal{F}$ are θ-angle-monotone when developed in the plane, for some $\theta < 90°$.

This step says, essentially, that each θ-monotone path Q' in the planar projection is not distorted much when lifted to $\mathcal{Q}$ on $\mathcal{C}$. This is obviously true as $\Phi \to 0$, but it requires proof. We need to establish that the left and right incident angles of the cut $\mathcal{Q}$ develop to the plane as still θ-monotone paths for some (larger) $\theta \leq 90°$.

First we bound the total curvature of $\mathcal{C}$ to address the phrase, "For sufficiently small Φ, ..." The near flatness of the convex cap $\mathcal{C}$ is controlled by Φ, the maximum tilt of the normals from $\hat{z}$. Let ω_i be the curvature at internal vertex $u_i \in \mathcal{C}$ (i.e., 2π minus the sum of the incident angles to u_i), and $\Omega = \sum_i \omega_i$ the total curvature. We bound Ω as a function of Φ in the following lemma. (The reverse is not possible: even a small Ω could be realized with large Φ.)

▶ **Lemma 4.** *The total curvature $\Omega = \sum_i \omega_i$ of $\mathcal{C}$ satisfies*

$$\Omega \leq 2\pi(1 - \cos\Phi) \approx \pi\Phi^2 - \pi\Phi^4/12 + O(\Phi^5) \ . \tag{2}$$

This is proved in the full version [13] as the area of a spherical cap on the Gaussian sphere for $\mathcal{C}$.

Our proof of limited curve lifting distortion uses the Gauss-Bonnet theorem,[3] in the form $\tau + \omega = 2\pi$: the turn of a closed curve plus the curvature enclosed is 2π.

To bound the curve distortion of Q', we need to bound the distortion of pieces of a closed curve that includes Q' as a subpath. Our argument here is not straightforward, but the conclusion is that, as $\Phi \to 0$, the distortion also $\to 0$:

▶ **Lemma 5.** *The difference in the total turn of any prefix of $\mathcal{Q}$ on the surface $\mathcal{C}$ from its planar projection Q' is bounded by $3\Delta_\perp + 2\Omega$ (Eq. 4), which, for small Φ, is a constant times Φ^2 (Eq. 5). Therefore, this turn goes to zero as $\Phi \to 0$.*

The reason the proof is not straightforward is that Q' could have an arbitrarily large number n of vertices, so bounding the angle distortion at each by $\Delta_\perp$ would lead to arbitrarily large distortion $n\Delta_\perp$. The same holds for the rim. So global arguments that do not cumulate errors seem necessary.

First we need a simple lemma, which is essentially the triangle inequality on the 2-sphere. Let $R' = \partial C$ and $R = \partial \mathcal{C}$ be the rims of the planar C and of the convex cap $\mathcal{C}$, respectively.

▶ **Lemma 6.** *The planar angle ψ' at a vertex v of the rim R' lifts to 3D angles of the triangles of the cap $\mathcal{C}$ incident to v, whose sum ψ satisfies $\psi \geq \psi'$.*

Now we use Lemma 6 to bound the total turn of the rim R of $\mathcal{C}$ and R' of C'. Although the rims are geometrically identical, their turns are not. The turn at vertex a' of the planar rim R' is $\pi - \psi'$, while the turn at vertex a of the 3D rim R is $\pi - \psi$. By Lemma 6, $\psi \geq \psi'$, so the turn at each vertex of the 3D rim R is at most the turn at each vertex of the 2D rim R'. Therefore the total turn of the 3D rim τ_R is smaller than or equal to the total turn of the 2D rim $\tau_{R'}$. And Gauss-Bonnet allows us to quantify this:

$$\tau_{R'} = 2\pi \ , \ \tau_R + \Omega = 2\pi \ , \ \tau_{R'} - \tau_R = \Omega \ .$$

For any subportion of the rims $r' \subset R'$, $r \subset R$, Ω serves as an upper bound, because we know the sign of the difference is the same at every vertex of r', r: $\tau_{r'} - \tau_r \leq \Omega$.

[3] See, for example, Lee's description [8, Thm.9.3, p.164]. My τ is Lee's κ_N.

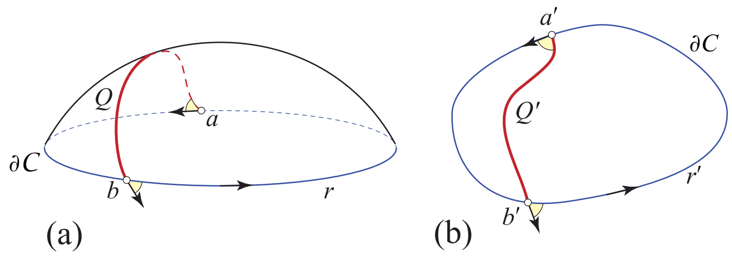

Figure 3 (a) C, the projection of the cap $\mathcal{C}$. (b) $\mathcal{Q}$ is the lift of Q' to $\mathcal{C}$.

6.1 Turn distortion of Q'

We need to bound $\Delta Q = |\tau'_Q - \tau_{\mathcal{Q}}|$, the turn difference between Q' in the plane and $\mathcal{Q}$ on the surface of $\mathcal{C}$, for Q' any prefix of an angle-monotone path in C that lifts to $\mathcal{Q}$ on $\mathcal{C}$. The reason for the prefix here is that we want to bound the turn of any segment of Q', not just the last segment, whose turn is $\sum_i \tau_i$. And note that there can be cancellations among the τ_i along Q', as we have no guarantee that they are all the same sign.

First we sketch the situation if Q cut all the way across $\mathcal{C}$, as illustrated in Fig. 3(a). We apply the Gauss-Bonnet theorem: $\tau + \omega = 2\pi$, where $\omega \leq \Omega$ is the total curvature inside the path $Q \cup r$, and then the planar projection (Fig. 3(b)), we have:

$$\begin{aligned} \tau + \omega &= \tau_Q + (\tau_a + \tau_b) + \tau_r + \omega = 2\pi \qquad (3) \\ \tau + \omega &= \tau_{Q'} + (\tau_{a'} + \tau_{b'}) + \tau_{r'} + 0 = 2\pi \end{aligned}$$

Subtracting these equations will lead to a bound on ΔQ.

But, as indicated, Q does not cut all the way across $\mathcal{C}$, and we need to bound ΔQ for any prefix of Q (which we will still call Q). Let Q cut from $a \in \mathcal{C}$ to $b \in \partial\mathcal{C}$. We truncate $\mathcal{C}$ by intersecting with a halfspace whose bounding plane H includes a, as in Fig. 4(a). It is easy to arrange H so that $H \cap Q = \{a\}$, i.e., so that H does not otherwise cut Q, as follows. First, in projection, Q' falls inside $\overline{W}(\theta, a')$, the backward wedge passing through a'. Then start with H vertical and tangent to this wedge at a, and rotate it out to reaching $\partial\mathcal{C}$ as illustrated. The result is a truncated cap $\mathcal{C}_T$. We connect a to a point c on the new $\partial\mathcal{C}_T$, depicted abstractly in Fig. 4(b). Now we perform the analogous calculation for the curve $Q \cup r_1 \cup ca$ on $\mathcal{C}$, and $\mathcal{Q}' \cup r'_1 \cup ca'$:

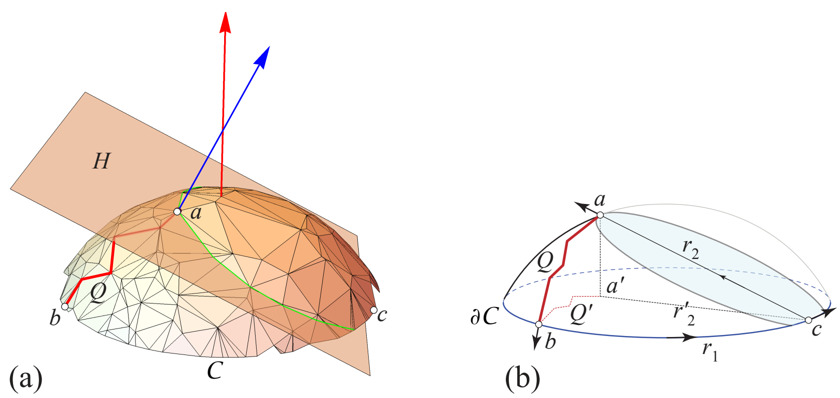

Figure 4 (a) Truncating $\mathcal{C}$ with H so that $H \cap \mathcal{Q} = \{a\}$. (b) $r_2 = ac$ and $r'_2 = a'c$.

$$\begin{aligned}\tau_{Q'} + (\tau_{a'} + \tau_{b'} + \tau_{c'}) + (\tau_{r'_1} + \tau_{r'_2}) + 0 &= 2\pi \\ \tau_{Q} + (\tau_{a} + \tau_{b} + \tau_{c}) + (\tau_{r_1} + \tau_{r_2}) + \omega &= 2\pi\end{aligned}$$

Subtracting leads to

$$\begin{aligned}\tau_{Q'} - \tau_{Q} &= ((\tau_a - \tau_{a'}) + (\tau_b - \tau_{b'}) + (\tau_c - \tau_{c'})) + (\tau_{r_1} - \tau_{r'_1}) + (\tau_{r_2} - \tau_{r'_2}) + \omega \\ \Delta Q &\leq 3\Delta_\perp + 2\Omega \qquad (4)\end{aligned}$$

The logic of the bound is: (1) Each of the turn distortions at a, b, c is at most $\Delta_\perp$. (2) The r_1 turn difference is bounded by $\omega \leq \Omega$. And (3) $\tau_{r_2} = \tau_{r'_2} = 0$. Using the small-$\Phi$ bounds derived earlier in Eqs. 1 and 2:

$$|\Delta Q| \leq 3\Delta_\perp + 2\Omega \approx (2\pi + \tfrac{3}{2})\Phi^2 . \qquad (5)$$

Thus we have $\Delta Q \to 0$ as $\Phi \to 0$, as claimed.

We finally return to the claim at the start of this section: For sufficiently small Φ, both sides L and R of each path $\mathcal{Q}$ of $\mathcal{F}$ are θ-angle-monotone when developed in the plane, for some $\theta < 90°$.

The turn at any vertex of $\mathcal{Q}$ is determined by the incident face angles to the left following the orientation shown in Fig. 3, or to the right reversing that orientation (clearly the curvature enclosed by either curve is $\leq \Omega$). These incident angles determine the left and right planar developments, L and R, of $\mathcal{Q}$. Because we know that Q' is θ-angle-monotone for $\theta < 90°$, there is some finite "slack" $\alpha = 90° - \theta$. Because Lemma 5 established a bound for any prefix of $\mathcal{Q}$, it bounds the turn distortion of each edge of $\mathcal{Q}$, which we can arrange to fit inside that slack. So the bound provided by Lemma 5 suffices to guarantee that:

▶ **Lemma 7.** *For sufficiently small Φ, both L and R remain θ-angle-monotone for some (larger) θ, but still $\theta \leq 90°$.*

To ensure $\theta \leq 90°$, we need that the maximum distortion fits into the acuteness gap: $|\Delta Q| \leq \alpha$. Using Eq. 5 leads to:

$$\Phi \leq \sqrt{\frac{2}{4\pi + 3}}\sqrt{\alpha} \approx 0.36\sqrt{\alpha} . \qquad (6)$$

For example, if all triangles are acute by $\alpha = 4°$, then $\Phi \approx 5.4°$ suffices.

That F lifts to a spanning forest $\mathcal{F}$ of the convex cap $\mathcal{C}$ is immediate. What is not straightforward is establishing the requisite properties of $\mathcal{F}$.

7 Radially monotone paths

> 4. Any planar angle-monotone path for an angle $\leq 90°$, is radially monotone, a concept from [11].

Let $Q = (v_0, v_1, \ldots, v_k)$ be a simple (non-self-intersecting) directed path of edges of C connecting an interior vertex v_0 to a boundary vertex $v_k \in \partial C$. We say that Q is *radially monotone* with respect to (w.r.t.) v_0 if the distances from v_0 to all points of Q are (non-strictly) monotonically increasing. We define path Q to be *radially monotone* (without qualification) if it is radially monotone w.r.t. each of its vertices: $v_0, v_1, \ldots, v_{k-1}$. It is an easy consequence of these definitions that, if Q is radially monotone, it is radially monotone w.r.t. any point p on Q, not only w.r.t. its vertices.

Before proceeding, we discuss its intuitive motivation. If a path Q is radially monotone, then "opening" the path with sufficiently small curvatures ω_i at each v_i will avoid overlap between the two halves of the cut path. Whereas if a path is not radially monotone, then there is some opening curvature assignments ω_i to the v_i that would cause overlap: assign a small positive curvature $\omega_j > 0$ to the first vertex v_j at which radial monotonicity is violated, and assign the other vertices zero or negligible curvatures. Thus radially monotone cut paths are locally (infinitesimally) opening "safe," and non- radially monotone paths are potentially overlapping.[4]

The condition for Q to be radially monotone w.r.t. v_0 can be interpreted as requiring Q to cross every circle centered on v_0 at most once; see Fig. 5. The concentric circles viewpoint makes it evident that infinitesimal rigid rotation of Q about v_0 to Q' ensures that $Q \cap Q' = \{v_0\}$, for each point of Q simply moves along its circle. Of course the concentric circles must be repeated, centered on every vertex v_i.

7.1 Angle-monotone chains are radially monotone

Fig. 5(c) illustrates why a θ-monotone chain Q, for any $\theta \leq 90°$, is radially monotone: the vector of each edge of the chain points external to the quarter-circle passing through each v_i. And so the chain intersects the v_0-centered circles at most once. Thus Q is radially monotone w.r.t. v_0. But then the argument can be repeated for each v_i, for the wedge $W(v_i)$ is just a translation of $W(\theta, v_0)$.

It should be clear that these angle-monotone chains are special cases of radially monotone chains. But we rely on the spanning-forest theorem in [9] to yield angle-monotone chains, and we rely on the unfolding properties of radially monotone chains from [11] to establish non-overlap. We summarize in a lemma:

[4] The phrase "radial monotonicity" has also appeared in the literature meaning radially monotone w.r.t. just v_0, most recently in [7]. The version here is more stringent to guarantee non-overlap.

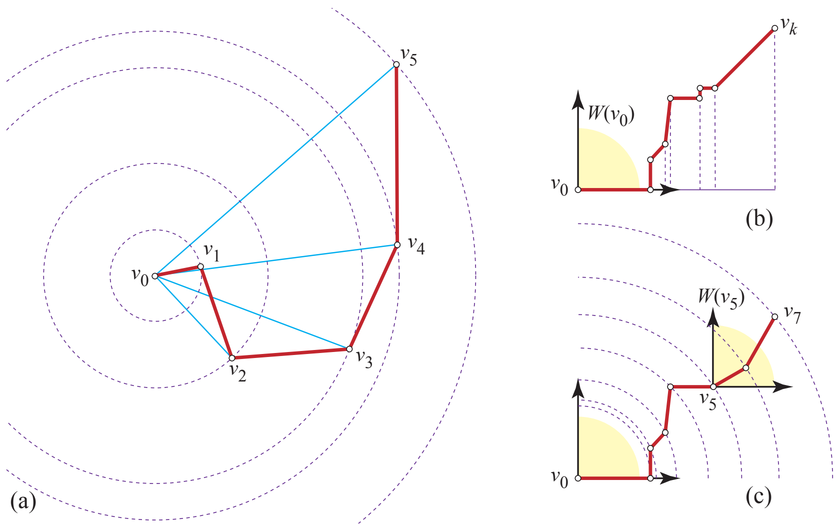

Figure 5 (a) A radially monotone chain, with its monotonicity w.r.t. v_0 illustrated. (b) A 90°-monotone chain, with x-monotonicity indicated. (c) Such a chain is also radially monotone.

▶ **Lemma 8.** *A θ-monotone chain Q, for any $\theta \leq 90°$, is radially monotone.*

8 Noncrossing L & R developments

5. Radial monotonicity of L and R, and sufficiently small Φ, imply that L and R do not cross in their planar development. This is a simplified version of a result from [11], and here extended to trees.

We will use $\mathcal{Q} = (u_0, u_1, \ldots, u_k)$ as a path of edges on $\mathcal{C}$, with each $u_i \in \mathbb{R}^3$ a vertex and each $u_i u_{i+1}$ an edge of $\mathcal{C}$. Let $Q = (v_0, v_1, \ldots, v_k)$ be a chain in the plane. Define the *turn angle* τ_i at v_i to be the counterclockwise angle from $v_i - v_{i-1}$ to $v_{i+1} - v_i$. Thus $\tau_i = 0$ means that v_{i-1}, v_i, v_{i+1} are collinear. $\tau_i \in (-\pi, \pi)$; simplicity excludes $\tau_i = \pm\pi$.

Each turn of the chain Q sweeps out a sector of angles. We call the union of all these sectors $\Lambda(Q)$; this forms a cone such that, when apexed at v_0, $Q \subseteq \Lambda(Q)$. The rays bounding $\Lambda(Q)$ are determined by the segments of Q at extreme angles; call these angles $\sigma_{\max}$ and $\sigma_{\min}$. See ahead to Fig. 6(a) for an example. Let $|\Lambda(Q)|$ be the measure of the apex angle of the cone, $\sigma_{\max} - \sigma_{\min}$. We will assume that $|\Lambda(Q)| < \pi$ for our chains Q, although it is quite possible for radially monotone chains to have $|\Lambda(Q)| > \pi$. In our case, in fact $|\Lambda(Q)| < \pi/2$, but that tighter inequality is not needed for Theorem 9 below. The assumption $|\Lambda(Q)| < \pi$ guarantees that Q fits in a halfplane H_Q whose bounding line passes through v_0.

Because $\sigma_{\min}$ is turned to $\sigma_{\max}$, we have that the total absolute turn $\sum_i |\tau_i| \geq |\Lambda(Q)|$. But note that the sum of the turn angles $\sum_i \tau_i$ could be smaller than $|\Lambda(Q)|$ because of cancellations.

8.1 The left and right planar chains L & R

Let ω_i be the curvature at vertex u_i of $\mathcal{Q}$. We view u_0 as a leaf of a cut forest, which will then serve as the end of a cut path, and the "source" of opening that path.

Let λ_i be the surface angle at u_i left of $\mathcal{Q}$, and ρ_i the surface angle right of $\mathcal{Q}$ there. So $\lambda_i + \omega_i + \rho_i = 2\pi$, and $\omega_i \geq 0$. Define L to be the planar path from the origin with left angles λ_i, R the path with right angles ρ_i. These paths are the left and right planar developments of $\mathcal{Q}$. We label the vertices of the developed paths ℓ_i, r_i.

Define $\omega(\mathcal{Q}) = \sum_i \omega_i$, the total curvature along the path $\mathcal{Q}$. We will assume $\omega(\mathcal{Q}) < \pi$, a very loose constraint in our nearly flat circumstances. For example, with $\Phi = 30°$, Ω for $\mathcal{C}$ is $< \pi\Phi^2 \approx 49°$, and $\omega(\mathcal{Q})$ can be at most Ω.

8.2 Left-of definition

Let $A = (a_0, \ldots, a_k)$ and $B = (b_0, \ldots, b_k)$ be two (planar) radially monotone chains sharing $x = a_0 = b_0$. (Below, A and B will be the L and R chains.) Let $D(r)$ be the circle of radius r centered on x. $D(r)$ intersects any radially monotone chain in at most one point. Let a and b be two points on $D(r)$. Say that a is *left of* b, $a \preceq b$, if the counterclockwise arc from b to a is less than π. If $a = b$, then $a \preceq b$. Now we extend this relation to entire chains. Say that chain A is *left of* B, $A \preceq B$, if, for all $r > 0$, if $D(r)$ meets both A and B, in points a and b respectively, then $a \preceq b$. If $D(r)$ meets neither chain, or only one, no constraint is specified. Note that, if $A \preceq B$, A and B can touch but not properly cross.

8.3 Noncrossing theorem

▶ **Theorem 9.** *Let $\mathcal{Q}$ be an edge cut-path on $\mathcal{C}$, and L and R the developed planar chains derived from $\mathcal{Q}$, as described above. Under the assumptions:*

1. *Both L and R are radially monotone,*
2. *The total curvature along $\mathcal{Q}$ satisfies $\omega(\mathcal{Q}) < \pi$.*
3. *Both cone measures are less than π: $|\Lambda(L)| < \pi$ and $|\Lambda(R)| < \pi$,*

then $L \preceq R$: L and R may touch and share an initial chain from $\ell_0 = r_0$, but L and R do not properly cross, in either direction.

That the angle conditions (2) and (3) are necessary is shown in the full version [13].

Proof. We first argue that L cannot wrap around and cross R from its right side to its left side. (Illustrations supporting this proof are in the full version [13].) Let $\rho_{\max}$ be the counterclockwise bounding ray of $\Lambda(R)$. In order for L to enter the halfplane H_R containing $\Lambda(R)$, and intersect R from its right side, $\rho_{\max}$ must turn to be oriented to enter H_R, a turn of $\geq \pi$. We can think of the effect of ω_i as augmenting R's turn angles τ_i to L's turn angles $\tau_i' = \tau_i + \omega_i$. Because $\omega_i \geq 0$ and $\omega(\mathcal{Q}) = \sum_i \omega_i < \pi$, the additional turn of the chain segments of R is $< \pi$, which is insufficient to rotate $\rho_{\max}$ to aim into H_R. (Later (Section 9) we will see that we can assume L and R are arbitrarily long, so there is no possibility of L wrapping around the end of R and crossing R right-to-left.)

Next we show that L cannot cross R from left to right. We imagine Q right-developed in the plane, so that $Q = R$. We then view L as constructed from a fixed R by successively opening/turning the links of R by ω_i counterclockwise about r_i, with i running backwards from r_{n-1} to r_0, the source vertex of R. Fig. 6(b) illustrates this process. Let $L_i = (\ell_i, \ell_{i+1}, \ldots, \ell_k)$ be the resulting subchain of L after rotations $\omega_{n-1}, \ldots, \omega_i$, and R_i the corresponding subchain of $R = (r_i, r_{i+1}, \ldots, r_k)$, with $\ell_i = r_i$ the common source vertex. We prove $L_i \preceq R_i$ by induction.

$L_{n-1} \preceq R_{n-1}$ is immediate because $\omega_{n-1} \leq \omega(\mathcal{Q}) < \pi$. Assume now $L_{i+1} \preceq R_{i+1}$, and consider L_i. Because both L_i and R_i are radially monotone, circles centered on $\ell_i = r_i$ intersect the chains in at most one point each. L_i is constructed by rotating L_{i+1} rigidly by ω_i counterclockwise about $\ell_i = \rho_i$; see Fig. 6(b). This only increases the arc distance between the intersections with those circles, because the circles must pass through the gap representing $L_{i+1} \preceq R_{i+1}$, shaded in Fig. 6(a). And because we already established that L cannot enter the R halfplane H_R, we know these arcs are $< \pi$: for an arc of $\geq \pi$ could turn $\rho_{\max}$ to aim into H_R. So $L_i \preceq R_i$. Repeating this argument back to $i = 0$ yields $L \preceq R$, establishing the theorem. ◀

Our cut paths are (in general) leaf-to-root paths in some tree $\mathcal{T} \subseteq \mathcal{F}$ of the forest, so we need to extend Theorem 9 to trees.[5] The proof of the following is in the full version [13].

▶ **Corollary 10.** *The $L \preceq R$ conclusion of Theorem 9 holds for all the paths in a tree $\mathcal{T}$: $L' \preceq R$, for any such L'. (See Fig. 6(c,d).)*

---

[5] This extension was not described explicitly in [11].

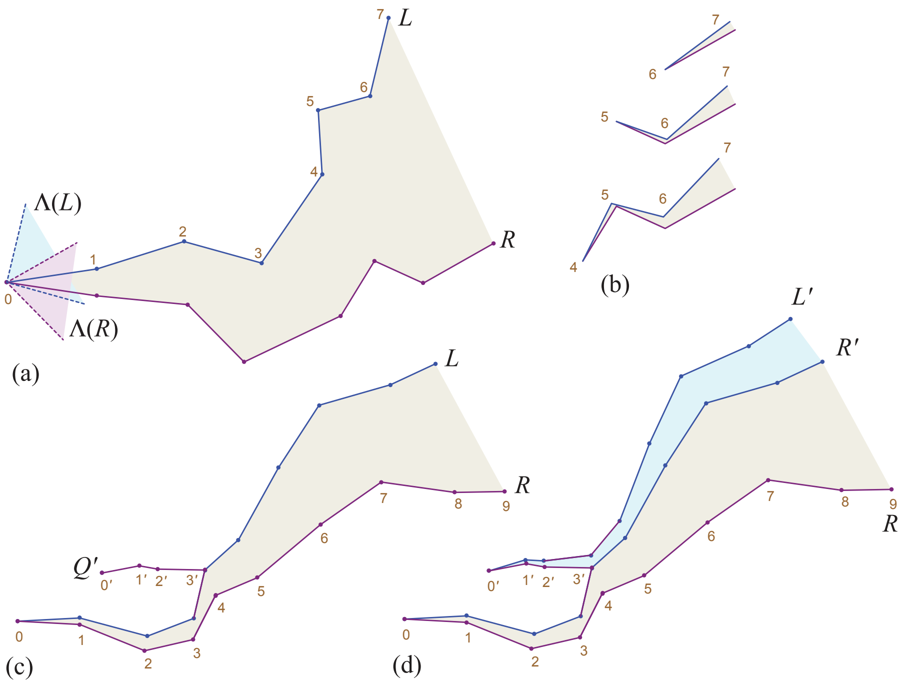

Figure 6 (a) Example 1: After opening Q to L and R. (b) Example 1: First steps in the induction proof. (c) Example 2: Q' joins Q at $v_3' = v_4$. After opening Q to L and R. (d) Example 2: After opening Q'.

9 Extending $\mathcal{C}$ to $\mathcal{C}^\infty$

6. Extending the cap $\mathcal{C}$ to an unbounded polyhedron $\mathcal{C}^\infty$ ensures that the non-crossing of each L and R extends arbitrarily far in the planar development.

In order to establish non-overlap of the unfolding, it will help to extend the convex cap $\mathcal{C}$ to an unbounded polyhedron $\mathcal{C}^\infty$ by extending the faces incident to the boundary $\partial\mathcal{C}$. The details are in the full version [13]. The consequence is that each cut path $\mathcal{Q}$ can be viewed as extending arbitrarily far from its source on $\mathcal{C}$. This technical trick permits us to ignore "end effects" as the cuts are developed in the next section.

10 Angle-monotone strips partition

7. The development of $\mathcal{C}$ can be partitioned into θ-monotone "strips," whose side-to-side development layout guarantees non-overlap in the plane.

The final step of the proof is to partition the planar C (and so the cap $\mathcal{C}$ by lifting) into strips that can be developed side-by-side to avoid overlap. We return to the spanning forest F of C (graph G), as discussed in Section 5.2. Define an *angle-monotone strip* (or more specifically, a θ-monotone strip) S as a region of C bound by two angle-monotone paths L_S and R_S which emanate from the quadrant origin vertex $q \in L_S \cap R_S$, and whose interior is vertex-free. The strips we use connect from q to each leaf $\ell \in F$, and then follow to the tree's root on ∂C. A simple algorithm to find such strips is described in the full version [13].

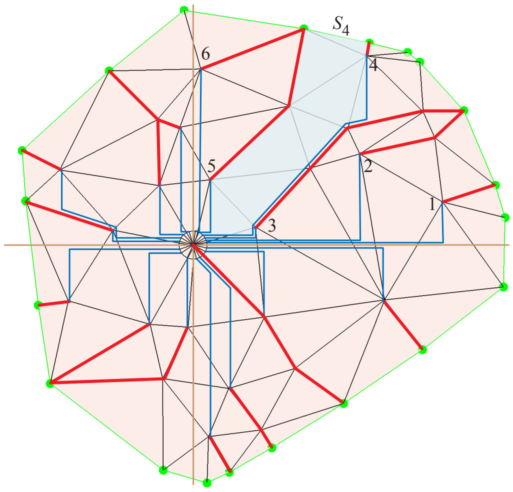

Figure 7 Waterfall strips partition. The S_4 strip highlighted.

see Fig. 7. Extending the $\preceq$ relation (Section 8.2) from curves $L \preceq R$ to adjacent strips, $S_i \preceq S_{i-1}$, shows that side-by-side layout of these strips develops all of $\mathcal{C}$ without overlap. This finally proves Theorem 1.

11 Discussion

It is natural to hope that Theorem 1 can be strengthened. That the rim of $\mathcal{C}$ lies in a plane is unlikely to be necessary: I believe the proof holds as long as shortest paths from q reach every point of $\partial\mathcal{C}$. Although the proof requires "sufficiently small Φ," limited empirical exploration suggests Φ need not be that small. (The proof assumes the worst case, with all curvature concentrated on a single path.) The assumption that $\mathcal{C}$ is acutely triangulated seems overly cautious. It seems feasible to circumvent the somewhat unnatural projection/lift steps with direct reasoning on the surface $\mathcal{C}$.

It is natural to wonder[6] if Theorem 1 leads to some type of "fewest nets" result for a convex polyhedron $\mathcal{P}$ [6, OpenProb.22.2, p.309]. At this writing I have a proof outline that, if successful, leads to the following (weak) result: If the maximum angular separation between face normals incident to any vertex leads to $\phi_{\max}$, and if the acuteness gap α accommodates $\phi_{\max}$ according to Eq. 6, then $\mathcal{P}$ may be unfolded to $\lesssim 1/\phi_{\max}^2$ non-overlapping nets. For example, $n = 2000$ random points on a sphere leads to $\phi_{\max} \approx 7.1°$ and if $\alpha \geq 6.9°$ – i.e., $\theta \leq 83.1°$ – then 64 non-overlapping nets suffice to unfold $\mathcal{P}$. The novelty here is that this is independent of the number of vertices n. The previous best result is $\lceil \frac{4}{11} F \rceil = \Omega(n)$ nets [14], where F is the number of faces of $\mathcal{P}$, which in this example leads to 1454 nets. However, the assumption that the acuteness gap α accommodates $\phi_{\max}$ restricts the applicability of this conjectured result.

References

1 Nicholas Barvinok and Mohammad Ghomi. Pseudo-edge unfoldings of convex polyhedra. arXiv:1709.04944: `https://arxiv.org/abs/1709.04944`, 2017.

2 Christopher J. Bishop. Nonobtuse triangulations of PSLGs. *Discrete & Comput. Geom.*, 56(1):43–92, 2016.

[6] Stefan Langerman, personal communication, August 2017.

3 Nicolas Bonichon, Prosenjit Bose, Paz Carmi, Irina Kostitsyna, Anna Lubiw, and Sander Verdonschot. Gabriel triangulations and angle-monotone graphs: Local routing and recognition. In *Internat. Symp. Graph Drawing Network Vis.*, pages 519–531. Springer, 2016.

4 Ju. D. Burago and V. A. Zalgaller. Polyhedral embedding of a net. *Vestnik Leningrad. Univ*, 15(7):66–80, 1960. In Russian.

5 Hooman Reisi Dehkordi, Fabrizio Frati, and Joachim Gudmundsson. Increasing-chord graphs on point sets. *J. Graph Algorithms Applications*, 19(2):761–778, 2015.

6 Erik D. Demaine and Joseph O'Rourke. *Geometric Folding Algorithms: Linkages, Origami, Polyhedra*. Cambridge University Press, 2007. `http://www.gfalop.org`.

7 Mohammad Ghomi. Affine unfoldings of convex polyhedra. *Geometry & Topology*, 18(5):3055–3090, 2014.

8 John M. Lee. *Riemannian Manifolds: An Introduction to Curvature*, volume 176. Springer Science & Business Media, 2006.

9 Anna Lubiw and Joseph O'Rourke. Angle-monotone paths in non-obtuse triangulations. In *Proc. 29th Canad. Conf. Comput. Geom.*, 2017. arXiv:1707.00219 [cs.CG]: `https://arxiv.org/abs/1707.00219`.

10 Joseph O'Rourke. Dürer's problem. In Marjorie Senechal, editor, *Shaping Space: Exploring Polyhedra in Nature, Art, and the Geometrical Imagination*, pages 77–86. Springer, 2013.

11 Joseph O'Rourke. Unfolding convex polyhedra via radially monotone cut trees. arXiv:1607.07421 [cs.CG]: `https://arxiv.org/abs/1607.07421`, 2016.

12 Joseph O'Rourke. Addendum to edge-unfolding nearly flat convex caps. arXiv:1709.02433 [cs.CG]: `http://arxiv.org/abs/1709.02433`, 2017.

13 Joseph O'Rourke. Edge-unfolding nearly flat convex caps. arXiv:1707.01006v2 [cs.CG]: `http://arxiv.org/abs/1707.01006`. Version 2, 2017.

14 Val Pincu. On the fewest nets problem for convex polyhedra. In *Proc. 19th Canad. Conf. Comput. Geom.*, pages 21–24, 2007.